Fuzzy Multiscale Region Growing for Segmentation of MR Images of the Human Brain

Karin Engel[1], Frederik Mauckscb[1], Anja Perlich[1], Matthias Wolff[1], Klaus Toennies[1], André Brechmann[2]

[1]Otto von Guericke University, Magdeburg, Germany
[2]Leibniz Institute for Neurobiology, Magdeburg, Germany
engel@isg.cs.uni-magdeburg.de

Abstract. We propose an automatic region growing technique for the segmentation of the cerebral cortex and white matter in MRI data. Our method exploits general anatomical knowledge and uses an iterative multi resolution scheme for the estimation of intensity distributions to compensate for artifacts within the data. We present a comparison to segmentation results created by the neuroimaging software Brainvoyager QX and show advantages of our approach based on a qualitative and quantitative evaluation.

1 Introduction

A precise segmentation of the cortical grey and white matter in anatomical MR images is necessary for a large number of medical applications, including morphometry, visualisation and the analysis of the functional organisation of the human brain as assessed by anatomical and functional MRI. An automatic segmentation of the cortex is difficult because the inter–subject variability of the human brain anatomy restricts the use of anatomical knowledge. Furthermore, image artifacts, such as noise, partial volume effects and inhomogeneities of the scans, complicate the separation between grey and white matter regions and also the identification of the boundaries of the cortex.

Several methods have been applied in recent years to estimate grey and white matter regions on MRI. The most popular methods separate intensity histograms which are assumed to be composed of distributions for the different tissue types. The data is then classified directly[1], or the parameters of the distributions determine the intensity range for region growing approaches [2]. Other methods include computationally expensive active contours and surfaces [3, 4, 5]. Here, the segmentation of thin gyral folds poses a problem due to partial volume effects and numerical issues (e.g., related with the curvature–based energy terms). In the presence of magnetic field inhomogeneities traditional region growing as well as active contours may underestimate, e.g. the upper part of the frontal lobe[6].

Our algorithm resolves the complex task utilising general anatomical knowledge. It combines an iterative region growing with fuzzy labels and estimation of the intensity distributions of the grey and white matter using a Gaussian

pyramid of the data. This multi resolution strategy allows to compensate for artifacts within the data and provides automatic, accurate and fast segmentations of the grey and white matter regions.

2 Fuzzy multiscale region growing

Our algorithm for separation of the cortical grey and white matter is based on a region growing, which uses histogram analysis for estimating the probability density functions (PDF) for the intensity of these different brain tissue types. The estimates are represented by Gaussian distributions P_ρ and P_ω, with $\mu_\omega > \mu_\rho$, and dynamically updated during a fuzzy region growing. The algorithm uses multiple scales of resolution of the data until the estimates for the inner and outer cortical surface (i.e. the grey–white matter boundary and pial surface) converge. The result of our algorithm is a segmentation in 3D where each voxel x of the 3D MRI data set is assigned one of three labels. These labels are l_ω for white matter, l_ρ for grey matter and l_b for background.

For segmentation we assume that the data sets are AC/PC–rotated such that pons and corpus callosum can be located in a set of sagittal slices. We further assume that the white matter is a single connected component, and is surrounded by the cortical grey matter which has an average thickness of $2.5 \pm 0.7mm$ [7]. For estimating the cortical grey matter based on the white matter, the cerebellum which is connected to the cerebrum via the brainstem, has to be removed.

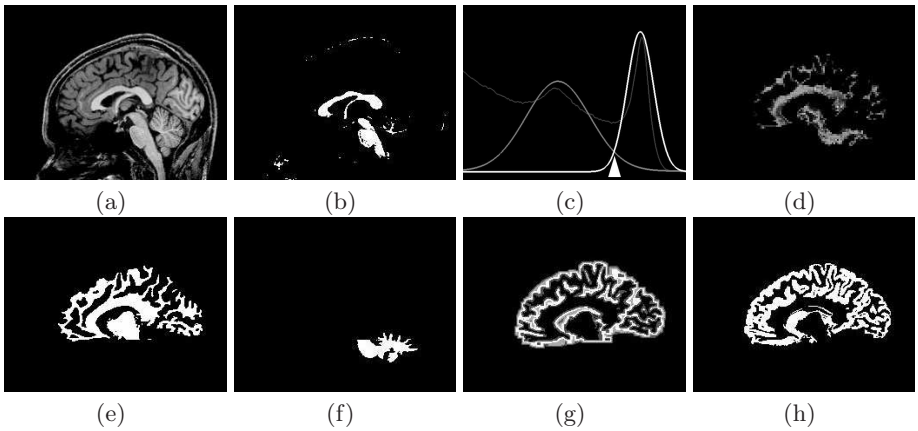

Fig. 1. Overview of the Fuzzy Multiscale Region Growing algorithm. (a) sagittal MR slice containing the interhemispheric fissure, (b) binarised version of (a), (c) histogram with estimated PDF P_ρ and P_ω, and threshold θ (arrow), (d) probability mask $\mathbf{P}_\omega$, (e) white matter segment W, (f) stripped cerebellum and brain stem, (g) probability mask $\mathbf{P}_\rho$ in terms of a normalised distance transform of W, (h) grey matter segment G.

2.1 Segmentation of the white matter

We obtain the desired seed points for the region growing within the white matter by selecting pixels that belong to the corpus callosum and pons (fig. 1(a)). Therefore, the sagittal slice that is most likely to contain the interhemispheric fissure is binarised using a threshold θ for separating grey and white matter (fig. 1(b)). Here, we use the grey value which represents the intersection of the estimated PDF, P_ρ and P_ω (fig. 1(c)). Seed points are obtained randomly by selecting points that survive a morphological erosion of the binarised volume.

Next, we compute a Gaussian pyramid $\{L(t), t = 0, ..., N\}$ of the data. A region growing is performed starting at lowest scale of resolution, $t = N$. The resulting segmentation is then propagated to the next scale in terms of a probability mask $\mathbf{P}_\omega(t)$, which determines for each voxel the probability of being included into the white matter region (fig. 1(d)). (Note that $\mathbf{P}_\omega(N) = 0$.) Therefore, the parameters μ and σ of the PDF, P_ω, are estimated by a histogram analysis at the current scale of resolution. We let

$$\hat{\mu} = \frac{1}{k} \sum_{i=1}^{k \leq K} h_i g_i(x), \hat{\sigma} = \frac{1}{K-1} \sum_{i=1}^{k \leq K} h_i (g_i(x) - \bar{g})^2, \tag{1}$$

given that grey value g_i occurs with frequency h_i. The $K = |\{x \in L(t) = l_\omega\}|$ samples are obtained by estimating an interval around the white matter PDF peak in the histogram. Here, we introduce a scaling factor $s \in \mathbb{R}$, such that $\hat{P_\omega} = sP_\omega$, and high values for s lead to less fuzzy segmentations of the white matter region. The result of this step is a binary mask, $W(x) = 1 \leftrightarrow x = l_\omega$ (fig. 1(e)).

2.2 Segmentation of the cortical grey matter

First, we use the AC/PC points to introduce a plug for separating the brainstem (truncus cerebri) and cerebellum from cerebrum using region growing (fig. 1(f)).

Based on a dilated version W_d of the white matter segmentation W, we calculate an approximated grey matter segment $G = W_d - W$, from which a random set of seed points is obtained for segmentation of the cortical grey matter. Here, we include a simplified model of the cortex thickness reported in [7] into the algorithm and use a normalised distance transform w.r.t. the grey–white matter boundary to initialise the probability mask $\mathbf{P}_\rho$ (fig. 1(g)). (Initially, the outer cortical surface is allowed to deviate by $4mm$ from the grey–white matter boundary.) Again, the parameters μ and σ of the PDF P_ρ are estimated by a histogram analysis based on samples from G, i.e. $K = |\{x \in L(t) = l_\rho\}|$ in equation 1. A fuzzy region growing based on these parameters results in the final grey matter segment, $G(x) = 1 \leftrightarrow x = l_\rho$ (fig. 1(h)).

3 Results

We evaluated the above algorithm using 20 MR data sets with (256^3) $1mm$ iso–voxels acquired on a 3 Tesla scanner. The quality of the data varied w.r.t.

signal–to–noise ratio and intensity inhomogeneities. For of a subset of 10 data sets, results of our algorithm have been compared with segmentations created by Brainvoyager QX (BVQX), a commercial software for the analysis of MRI (`http://brainvoyager.com`). These segmentations have been created with interaction by an experienced user and are more exact than an automated segmentation using BVQX. Segmentation includes rotation of the data into the AC/PC–plane, inhomogeneity correction, isolation of the cerebrum by applying standard masks, spatial smoothing, region growing (using a user–specified threshold θ) and morphological operations[2]. Note that our algorithm was also applied to the AC/PC–rotated data to allow for a comparison of both methods.

Examples of segmentation results using both algorithms are given in figure 2. A visual inspection by neurobiologists suggests that the grey–white matter boundary found by our algorithm is usually more exact, especially in regions of low contrast, e.g. the lower temporal lobe (figs. 2(g), 2(h)) and occipital lobe. Overall, the BVQX segmentations underestimate the white matter and miss white matter of gyri which can be easily identified (figs. 2(e)-2(h)). Since the outer cortical surface given by the commercial software is simply an estimate based on a the grey–white matter boundary and average cortex thickness of $3mm$, the results are usually inexact. Again, a visual inspection proved the correctness of our results.

For a quantitative analysis we used a set of manually labelled landmarks in visual and auditory regions as ground truth. These anatomical landmarks

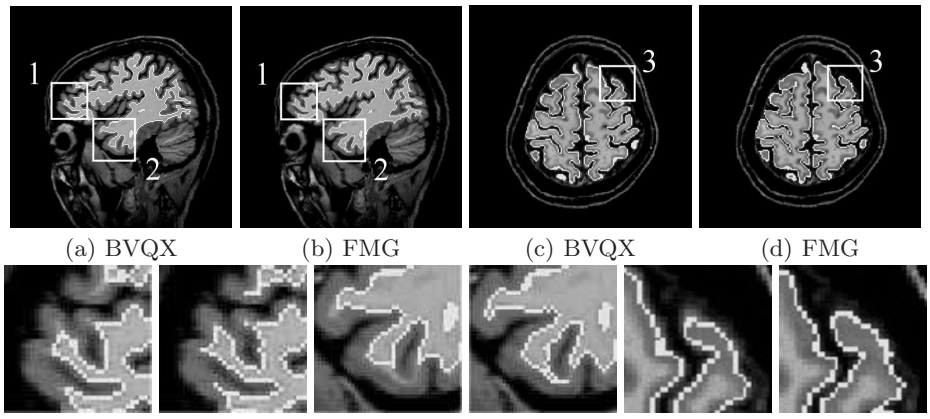

(a) BVQX (b) FMG (c) BVQX (d) FMG

(e) BVQX:1 (f) FMG:1 (g) BVQX:2 (h) FMG:2 (i) BVQX:3 (j) FMG:3

Fig. 2. Comparison of segmentation results using BVQX and our proposed algorithm (FMG). Note the underestimation of the white matter in the BVQX results. Differences in the resulting inner cortical surface (a-b) are visible in the enlarged areas within the frontal (1) and lower temporal lobe (2) in (e-h). While our algorithm actually segments the cortical grey matter, BVQX computes an estimate by constant dilation of the white matter segmentation. The resulting outer cortical surfaces (c-d) are usually less exact for the BVQX segmentations, as visible in the frontal lobe (3) in (i).

contribute to the inner cortical surface, λ_i (voxels within the grey matter that border white matter) and outer cortical surface, λ_o (background voxels that border grey matter). Our segmentations identified at average an absolute distance of $\delta = 0.37 \pm 0.74mm$ and a maximum distance of $d = 5.91mm$ to the ground truth λ_i (BVQX: $\delta = 1.3 \pm 1.18mm, d = 8.37mm$), and $\delta = 1.15 \pm 1mm$, $d = 5.83mm$ for the ground truth λ_o (BVQX: $\delta = 1.43 \pm 1.3mm, d = 7.07mm$).

Our algorithm requires no user interaction, and due to the multi resolution strategy the same set of parameters ($s = 1.0, N = 5$) could be used for all data sets without the need for further pre–processing, e.g. inhomogeneity correction. A visual inspection of segmentation results in 10 uncorrected MR data sets suggests that even in the presence of strong magnetic field inhomogeneities our algorithms gives satisfactory results. In contrast, using the BVQX software, small variations in the parameter values led to significant alterations in the segmentations, while segmentation failed in the uncorrected data sets. The computational time of our algorithm on a data set is about 68 seconds (3GHz Core2Duo, 4Gb RAM), which clearly outperforms the semi–automatic segmentation process with BVQX.

4 Discussion

We presented a region growing approach for the accurate and fast segmentation of cortical grey and white matter in MRI data. The proposed algorithm does not require any user interaction, and utilises an iterative multi resolution scheme which makes parametrisation of the region growing more robust. A visual inspection by neurobiologists and quantitative evaluation confirmed the accuracy in the estimated cortical surfaces.

Acknowledgement. The authors would like to thank Andreas Fügner and Jochem Rieger for providing the segmentation results used in this study.

References

1. Mangin J, et al. Robust brain segmentation using histogram scale-space analysis and mathematical morphology. Proc MICCAI. 1998; p. 1230–1241.
2. Kriegeskorte N, Goebel R. An efficient algorithm for topologically correct segmentation of the cortical sheet in anatomical MR volumes. Neuroimage. 2000;14:329–346.
3. Davatzikos C, Bryan N. Using a deformable surface model to obtain a shape representation of the cortex. IEEE Trans Med Imaging. 1996;15(6):785–795.
4. Dale A, et al. Cortical surface–based analysis 1. segmentation and surface reconstruction. Neuroimage. 1999;9:179–194.
5. Goldenberg R, et al. Cortex segmentation: A fast variational geometric approach. IEEE Trans Med Imaging. 2002;21(12):1544–1551.
6. Sokoll S, et al. Dynamic segmentation of the cerebral cortex in MR data using implicit active contours. Proc MIUA. 2008; p. 184–188.
7. Fischl B, Dale A. Measuring the thickness of the human cerebral cortex from magnetic resonance images. Proc Nat Acad Sci. 2000;97:11044–11049.